https://doi.org/10.2352/ISSN.2470-1173.2017.6.MOBMU-308

Comparative visualization of the geometry of a hollow box girder using 3D-LiDAR – Part 2: Reconstruction of 3D Geometric Model

Stefan Maack[1], Jenny Knackmuß[2], Reiner Creutzburg[2]
[1] BAM Bundesanstalt für Materialforschung und -prüfung, D-12205 Berlin, Germany
[2] Brandenburg University of Applied Sciences, Department of Informatics and Media, PO Box 2132, D-14737 Brandenburg, Germany

Abstract

With the mandatory introduction of the May 2011 directive for reassessment of bridges in Germany, the administrations of the federal and state governments have the duty to prove the stability of their bridge stock. Verification of bridge stability will be realized with consideration of the newly increased traffic loads. Particularly in older bridges, the verification can only be achieved if calculative surplus load capacity of the original structural design is taken into account in the recalculation. One option for considering these reserves is the exact determination of the dead weight of the bridge. Within this case study, it will be demonstrated how the problem can be practically solved.

In order to determine the dead weight of a concrete bridge, its volume has to be calculated. as a first step, a 3D laser scanner is used to record the internal geometry of a hollow box bridge girder. For the determination of the thickness of the concrete member, the non-destructive technique ultrasonic echo is applied. The construction must be segmented in approximately equidistant parts in order to be able to carry out an economic and efficient investigation. The description of the segmentation of the point cloud, carried out in a 2D model, was presented in the first part of the publication. The subject of this presentation is the merging of 2D cross sections into a 3D model, from which the weight of the bridge can be calculated.

Introduction

A guideline [1] was introduced in Germany five years ago according to which the stability of older bridge structures must be demonstrated, taking into account the increased traffic loads and its effects on the bridge structures. The current traffic loads are partly higher compared to the load assumptions of the older regulations. For example, transport of goods in the years 1980 to 2010 has almost increased by a factor of 15 [2]. In Germany, about 39,000 bridges are affected by this review. The bridges with the highest risk of instability are those constructed between the years 1950 and 1970. With a life span of about 45 years, these structures have reached the end of their anticipated service life. Furthermore, during this time, materials were used which, according to our current knowledge, are classified as problematic concerning durability. As a result, around 2,400 structures were identified as having a high prioritization for the re-calculation. These bridges are investigated first.

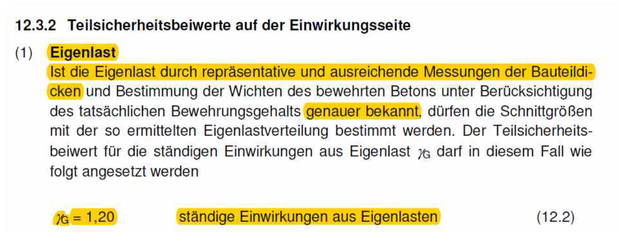

12.3.2 Teilsicherheitsbeiwerte auf der Einwirkungsseite

(1) **Eigenlast**
Ist die Eigenlast durch repräsentative und ausreichende Messungen der Bauteildicken und Bestimmung der Wichten des bewehrten Betons unter Berücksichtigung des tatsächlichen Bewehrungsgehalts genauer bekannt, dürfen die Schnittgrößen mit der so ermittelten Eigenlastverteilung bestimmt werden. Der Teilsicherheitsbeiwert für die ständigen Einwirkungen aus Eigenlast γ_G darf in diesem Fall wie folgt angesetzt werden

$\gamma_G = 1{,}20$ ständige Einwirkungen aus Eigenlasten (12.2)

Figure 1: Section from the guideline with regard to the reduction of the safety factors of the dead weight [1].

The enacted guideline provides the engineers with various possibilities of structural calculation. A particularly interesting aspect here is the possibility of reducing the safety factors, which were taken into account during the calculation. Through this reduction, the load-bearing capacity of the bridge can be taken into account. A special focus is on the calculation of the dead load of bridge structures. The guideline says that the safety factor can be reduced from $\gamma_G = 1.35$ to $\gamma_G = 1.20$ [1], as shown in Figure 1. This corresponds to a possible calculative reserve of 15% of the dead weight of the bridge, which counteracts to the increased stress caused by traffic.

In order to be able to estimate the possible potential of the calculative reserve, a realistic example is given below [3]. This is a model calculation of a double webbed tee-beam bridge with two lanes per direction. The cross section is shown in Figure 2, the longitudinal profile in Figure 3. The dead weight of the structure is about 790 t (790 t ≈ 870 tn. sh.) for a section with a length of 32.0 m. The possible maximum reserve applied in the calculation of the origin thus amounts to 118 t (118 t ≈ 131 tn. sh.) for such a section.

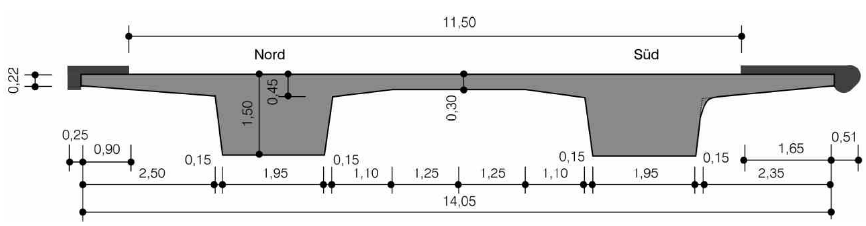

Figure 2: Schematic representation of the cross of the example calculation in [3].

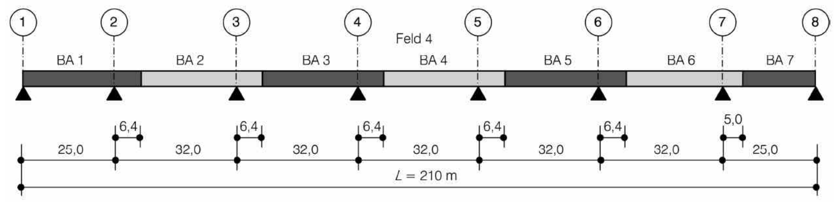

Figure 3: Schematic representation of longitudinal profile of the example calculation in [3].

The given example shows very well how significant the potential of the determination of the dead weight can be for a recalculation. However, the guideline [1] does not specify how to exactly determine of the dead weight. It says: *"(...) If the dead weight is more precisely determined by representative and sufficient measurements of the thickness of the structural element (...), it may be stated as follows (...)"* Figure 1, highlighted text). The term "*representative* and *sufficient measurement"* is not specified.

The research performed [4] demonstrated how such a calculation of the dead weight can be carried out using non-destructive testing methods. In the first part of this publication, "Comparative visualization of the geometry of a hollow box girder using 3D-LiDAR – Part 1: Cross sectional area" [5], various possibilities for determining the dead weight are discussed. Due to the special boundary conditions on the bridge construction, a combination of different test methods is used. The necessary different steps are described in [5] and once again summarized in a process flow chart in a schematic view in Figure 4.

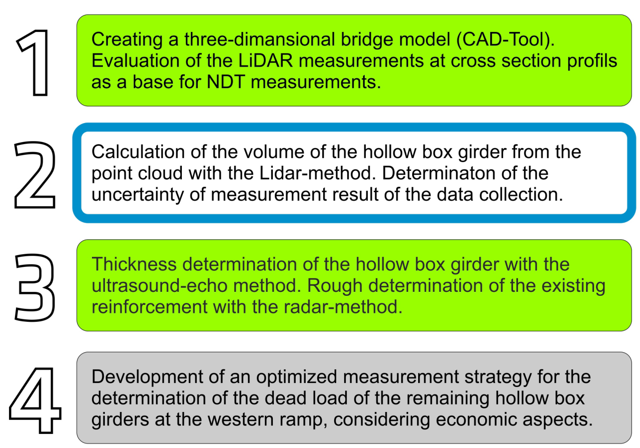

Figure 4: Presentation of the basic steps of the research work to determine the dead weight of the bridge (in accordance with [3], green - finished, blue edged - in process, gray - partly completed).

The bridge, which was investigated in the frame of the research project, spans over the river Elbe in Hamburg (Köhlbrandbrücke). The bridge is one of the most important connections to the container port. The bridge structure is divided into three areas consisting of two ramps and the cable-stayed bridge that spans the river. The cable-stayed bridge is a steel structure. The ramps are constructed of prestressed concrete. A detailed description of the geometric dimensions and constructional elements of the structure can be found in the first part of this publication [5]. The examined area of the western ramp between the pier 107 and pier 106 of the bridge is shown in an overview in Figure 5.

The determination of the dead weight of the bridge was carried out by an exemplarily evaluation of a representative area of the bridge structure. This region between the piers 106 and 107 is identified in Figure 5. This type of constructional design is referred to as a hollow box girder. Subsequently, the strategy developed here must be applied respectively to the other areas of the bridge's western ramp (Step 4, Figure 4).

Figure 5: Overview of the research area at the western ramp of the Köhlbrandbrücke.

In the first part of the research project, the basic procedure for solving the problem is described. For this purpose, a multi-stage procedure was established in consultation with the project partners [5]. The described intermediate steps and their processing status are shown schematically in Figure 4. In Step 1, data collection and a first evaluation of the LiDAR measurements took place. The calculation of the volume of the inner hollow box girder (Step 2), taking into account the measurement uncertainties as the basis for the evaluation of the non-destructive testing (NDT) measurements, is carried out as part of this presentation. The determination of the structural thicknesses as well as the position of the internal structural elements (for example, reinforcement) using the NDT methods are the subjects of Step 3. Subsequently, the dead weight of the hollow box girder can be determined under indication of the measurement uncertainty. The NDT measurements and their evaluation have already been completed. In Step 4, an overarching strategy for investigations should be developed across the entire western ramp.

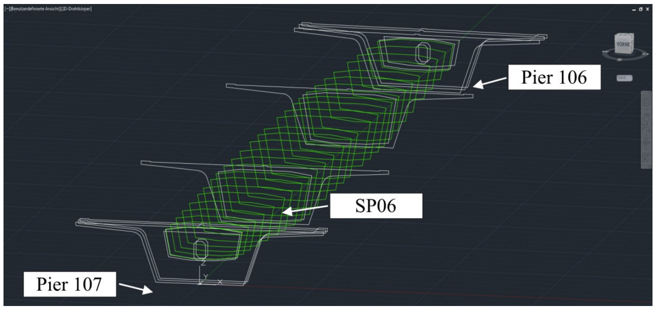

Figure 6: CAD drawing of various cross sections of the bridge (white lines). Green colored lines represent the 27 positions of the NDT measurements [5].

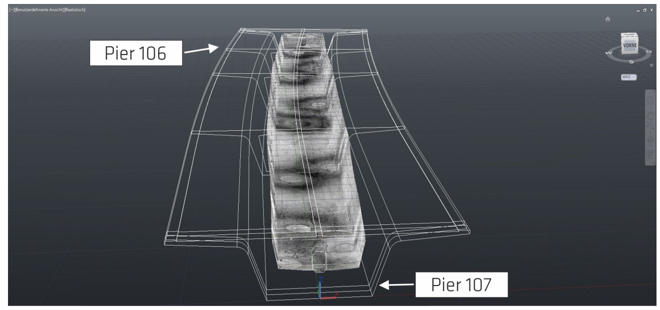

Figure 7: Representation of the point cloud measured by the LiDAR method faded into the bridge model drawn with CAD.

In the following, the most important results of Step 1 of the evaluation from [5] are summarized again and presented graphically. The calculation of the volume is ultimately necessary for the calculation of the dead weight of the hollow box girder. The volume should be determined from the combination of the LiDAR measurements and the NDT measurements. With the NDT methods, the reinforcement at the inner construction and the thickness of the structural elements can both be detected [6,7,9,10]. The NDT measurements for the determination of the thickness of the walls of the hollow box girder were carried out at 27 measuring positions. The different measuring positions have a separation distance of approximately 2.5 m. In Figure 6, the different positions are indicated by green lines. The LiDAR measurements determine the real geometrical dimensions of the structure at these positions.

In the first step, segments were extracted from the point cloud at these 27 positions. The point cloud of the LiDAR measurement is shown in Figure 7 within the CAD drawing. The segmentation of the point cloud was carried out by an algorithm implemented in Matlab©. In order to obtain a sufficient number of measuring points, an additional range of ± 50 mm is recorded next to the cutting plane of the cross section profile. Since the hollow box girder changes its geometry along its longitudinal axis, the segmentation is done in two steps. In the first step, the straight section of the hollow box is segmented, Figure 8 (green area), and in the second step the clothoid section, Figure 8 (blue area). It should be noted that the radius changes at each segment of the section of the clothoid. Figure 8 shows the two sections as well as the extracted 27 segments (blue lines) of the point cloud in different perspectives in an overview. In the upper part of Figure 8, the segmented cross-sections are shown in a 3D representation. The flat projection of the segments as well as the geometric shape of the hollow box (green-blue dashed line) can be seen in the lower part of the Figure.

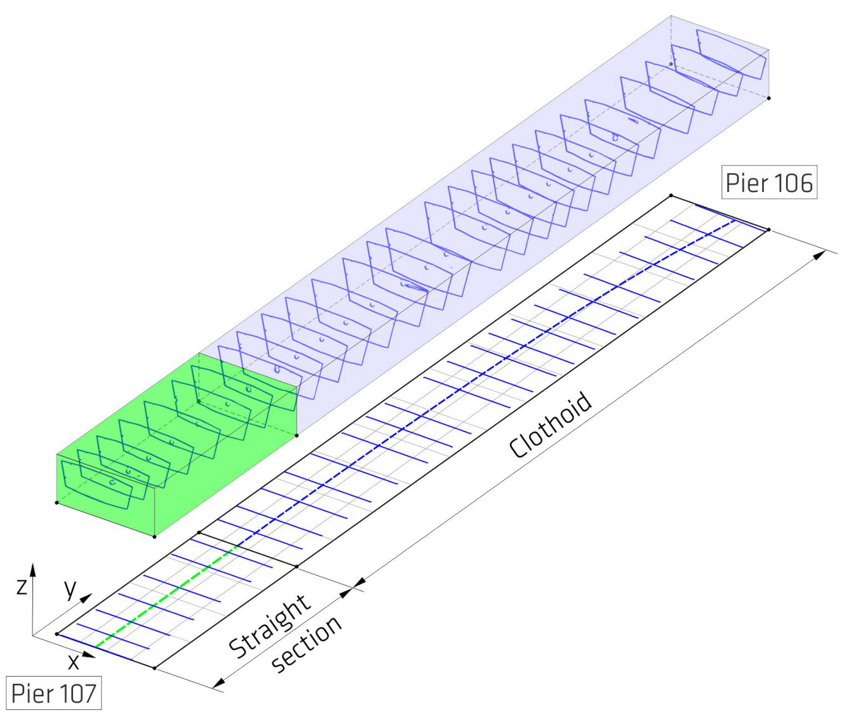

Figure 8: Illustration of the 27 segments extracted from the point cloud at the positions where NDT measurements were carried out. The section of the investigated structure is divided into a straight (green section) and a clothoidal section (blue area).

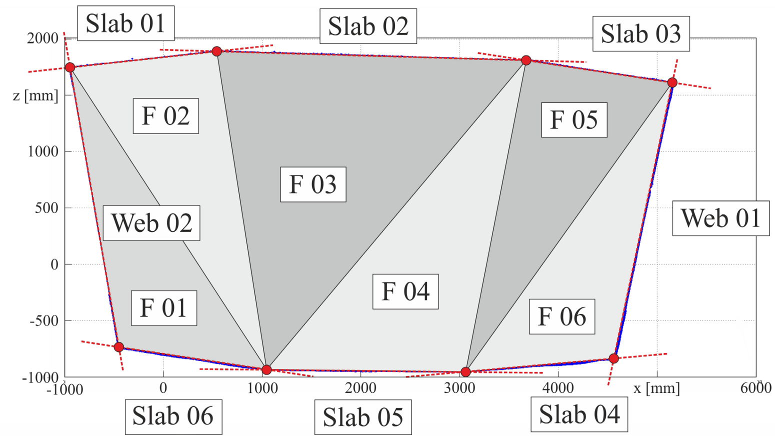

Figure 9: Results from [5] of a reconstructed cross-section profile by linear regression of the component geometry.

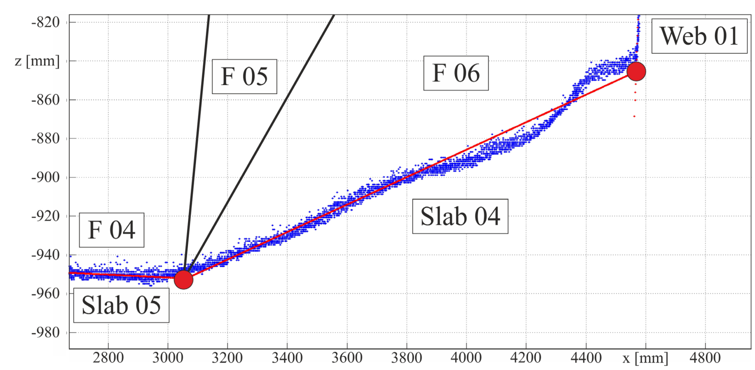

Figure 10: Representation of the surface of the concrete (blue points - LiDAR) at a selected typical position of the structure (figure from [5]).

In order to easily convert the different segments of the point cloud into a 2D model, it is necessary to transform the points of the segments into a planar surface. Through this transformation, it is then very easy to create a 2D model of the cross-sectional area by linear regression. The transformation can now be used to calculate the area for each cross-section of the 27 segments. Figure 9 [5] shows how the surface is reconstructed through linear regression at the component boundaries. Subsequently, the total area of the cross-section profile is calculated by adding the triangular partial surfaces. This basic approach has already been published in the first part of this publication [5].

In the first part of the project [5], a model was introduced in which the highly varying topography of the concrete surfaces could be described in a 2D model. Since this factor plays a central role in the later calculation of the internal volume of the hollow box girder, the chapter, "Surface of the concrete - deduction of a distribution function", is discussed in more detail below.

2D-modelling of cross-sectional profile from the point cloud

It may be necessary to use so-called probabilistic calculation methods to recalculate bridges [12]. To be able to use these calculation methods, the probability of loading effects must be specified for each parameter applied [7]. This is usually done by specifying the probability density function. In the calculation of the dead weight of the bridge element presented here, these examples follow:

- Uncertainty of measurement of LiDAR,
- Uncertainty of measurement of NDT-methods,
- Distribution of the bulk density of the concrete,
- Deviations from the planed building geometry, such as the roughness of the concrete surface,
- Number and distribution of reinforcement.

For the calculation of the internal volume with respect to the distribution function, some explanations are given below for the imperfections of the component surfaces and the uncertainty of measurement of the LiDAR-method.

Surface of concrete – deduction of a distribution function

Due to the technologically demanding processes involved in the production of concrete structures, deviations in the geometry of the construction usually occur. This concerns both the required thicknesses of the components as well as the shape of the surface. A representative example of such a surface can be seen in Figure 10 from [5]. The figure shows very clearly that there is a difference between a 2D model created by a linear regression (red straight line) and reality (blue points). To take into account these deviations in the 2D model, the introduction of a related standard deviation was proposed in [5]. The purpose of this approach is to illustrate the real conditions of the structure.

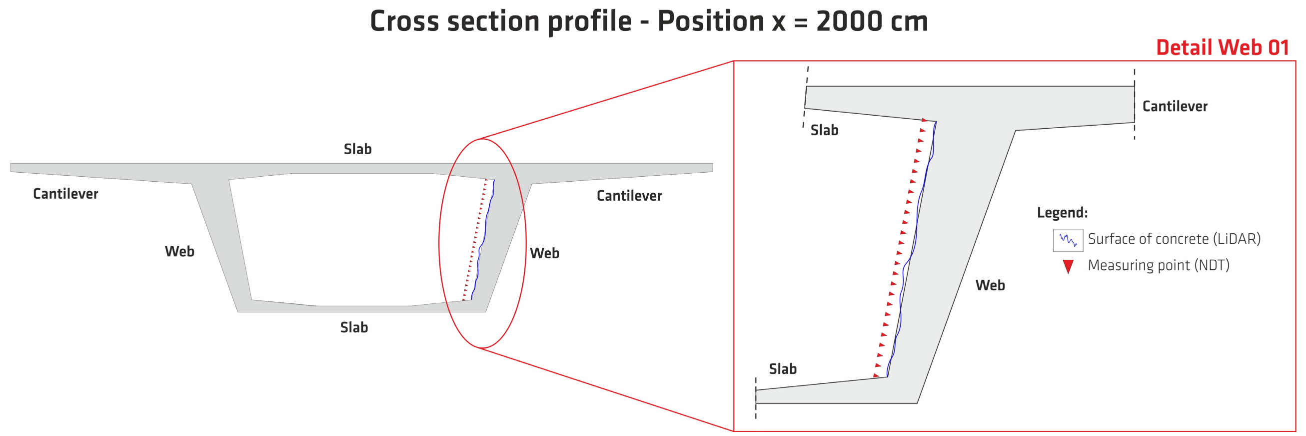

Figure 11: Schematic representation of the inner area of the hollow box and the available conditions during the measurement with the NDT methods.

Figure 11 shows the schematic representation of the conditions inside the hollow box girder. Due to the technological conditions in the construction of the structure, the surfaces are not exactly flat, as shown in Figure 10. The deviations from the target state are indicated by a blue dotted line in the Figure 11. Furthermore, the points at which the ultrasonic measurements for the determination of the construction thickness are performed are represented by red triangles. The number of triangles in Figure 11 is not the actual number. The manual ultrasonic measurements were carried out with an offset of the measurement points of 5 cm, Figure 12. If the boundary conditions were as shown in Figure 11, the structural thickness and, consequently, the weight of the bridge could be calculated directly. In fact, the calculation is more complicated due to the influence of the NDT measurements of the thickness.

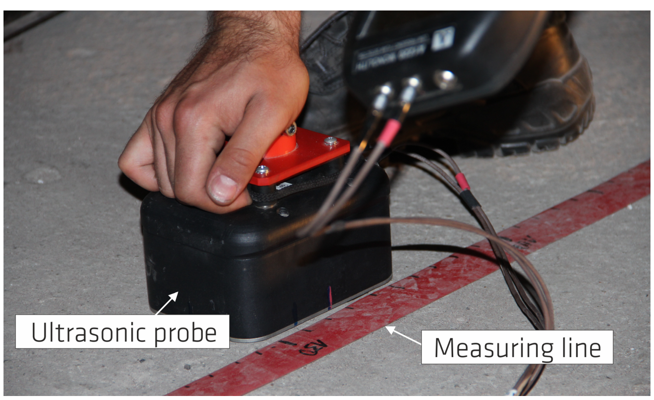

Figure 12: Determination of the thickness of the component by ultrasonic echo measurements with an offset of the measuring points of 5 cm.

An example of the NDT results for material thickness is shown in Figure 13. This figure shows typical results from an ultrasonic measurement of wall thickness. This is a color-coded signal image, typical known as B-scan. The measurement takes place on the inside of the hollow box girder. A short sound pulse is sent into the component with an ultrasound probe. The pulse is then reflected at the outside of the building. As a result of the pulse's measured travel time and the calibrated sound velocity, the construction thickness can then be calculated at each measuring point.

It is now easy to see that the outer side of the structure can not be determined at every measuring point of the ultrasonic measurements. In the color-coded B-scan, it can be seen that in some areas, the ultrasound signal no longer exists or there is an apparent displacement of the outer wall. These measurement points are now indicated by gray triangles in Figure 13. The possible reasons for ultrasound signals not being received at these positions are diverse due to the fact that structural elements are located in the interior of the building part. As an example, see Figure 13 the tendons represented by blue dots. These tendons are often installed in several layers. This has the consequence that the ultrasonic signals will be shadowed by these tendons. The outer side of the wall can thus no longer be detected. In addition to structural elements, however, problems with sound excitation at the surface, which could be caused by coatings or cracks near the surface, can also lead to improper receiving of signals. This means that calculating the structural thickness can have random errors.

What does this mean for 2D modeling of the cross section profile? Due to the random character of whether or not the thickness of the building was determined at a measuring position, a direct calculation is very difficult to achieve. Therefore, the idea is to simplify, by representing the structural component boundaries as straight lines. In addition, the deviation from this straight line must also be determined mathematically. For the inner region of the girder, this is the variance resulting from the topography of the surface of the concrete and the uncertainty of measurement of the LiDAR-System.

How this deviation is determined for the inner region is shown in Figure 13 in a simplified schematic illustration. In the first step, a linear regression function is generated (compare Figure 10 (red line)). The deviations from this straight line are indicated by red and green areas. These depict the actual surface of the concrete. If the regions are represented in a diagram in the form of a frequency distribution, a probability density function can very easily be determined from this, as shown in Figure 13 on the left side. With this distribution function, further calculations can now be carried out without disregarding the relevant geometric information. The 2D model, which is determined in this way, gives a relatively good approximation of the real conditions of the structure.

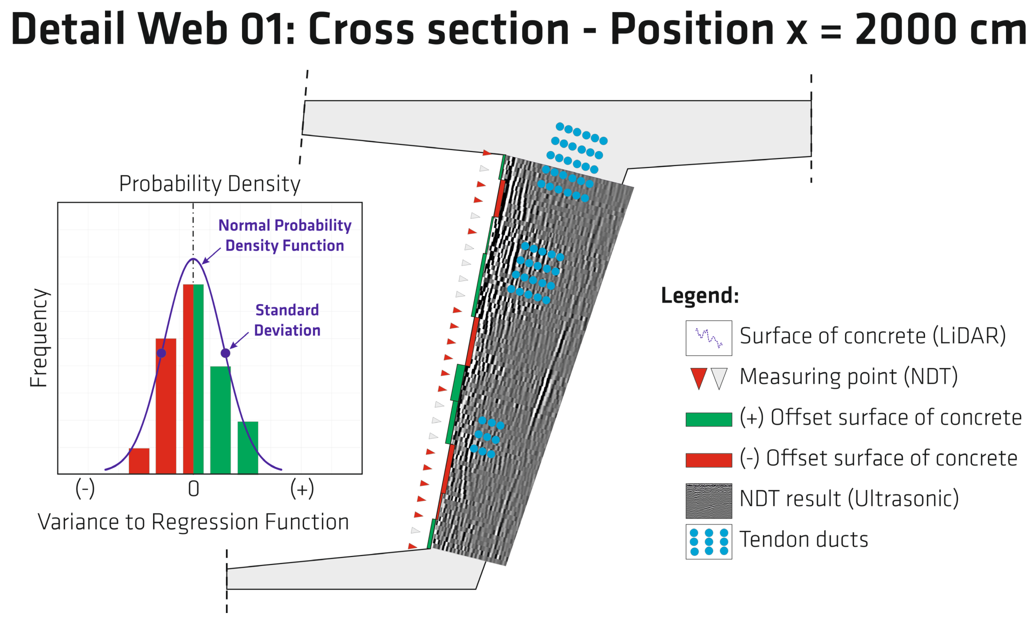

Figure 13: Schematic representation of the real conditions in the determination of the constructional thickness of the hollow box girder by NDT measurements and the resulting consequences.

Uncertainty of LiDAR

Investigations on the uncertainty of LiDAR measurement have not yet been completed. According to the manufacturer of the measurement technique, the uncertainty of measurement can be assumed with an accuracy of ±1 mm. For further calculations, it is assumed that this is the standard deviation. The extent to which this information is sufficient as a basis for the calculation of a bridge is to be determined through future testing. In particular, this parameter does not take into account that the bridge is continuously deformed during the measurements. The deformations can be in the centimeter range for constructions under external loads, such as traffic or wind loads. The deformations presumably have a considerable influence on the result of measurement.

For further calculations, a value for the uncertainty of measurement of ±2 mm is assumed. In order to estimate the influence of the uncertainty of measurement on the calculation in a first approximation, different scenarios with varying uncertainties of measurement are calculated in the chapter *Estimation of the influence of the uncertainty of LiDAR measurements on the volume calculation*.

Calculation of the inner surfaces of the cross section profiles with the Monte Carlo simulation

The following chapter explains how inner surfaces can be calculated by considering the distribution functions. For the calculation of the internal total area, the cross-section profile is subdivided into triangular surfaces, Figure 9. Various possibilities are considered for the calculation. Figure 14 shows exemplarily the boundary conditions for the calculation of a triangular surface. In [5] the largest possible deviation was taken into account for the calculation of the area in a first approximation. In order to obtain a more accurate result, there is the possibility of a mathematically analytical calculation of the surfaces. Another possibility is to carry out a Monte Carlo simulation.

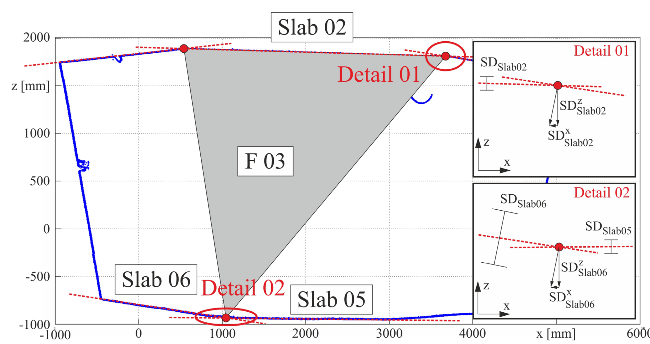

Figure 14:Representation of the straight lines formed by linear regression, giving the related standard deviation for the cross profile SP06 from [5].

Within the scope of this research work, the internal area was calculated using such a simulation. The Monte-Carlo simulation is a mathematical procedure from the field of stochastics. In this simulation, a problem is solved numerically using the probability theory. In this way, a large number of random events is calculated by a computer. In this case, the random events are the mathematical description of the surface of the concrete by a distribution function and the uncertainty of measurement of the LiDAR method. The calculation of the inner surface as well as the calculation of the inner volume of the hollow box girder can, therefore, be carried out very well with this simulation. As a result of the simulation, a large number of values are obtained from which an empirical distribution function can be determined. These results are then the basis for the recalculation of bridges using probabilistic methods [7,12].

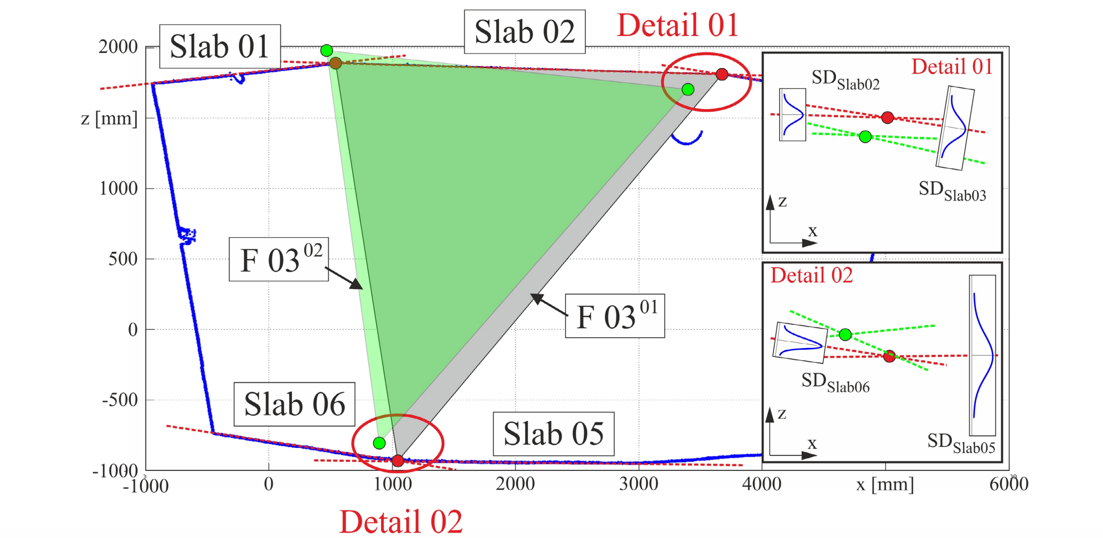

Figure 15: Schematic representation of the influence of the displacement of the calculated intersection points on the newly developing surface (green).

The basic procedure for calculating the inner surface using the determinant equation is shown in [5]. Based on this, the programming of the Monte-Carlo simulation follows. The simulation is implemented in Matlab©. In the first step of the simulation, the calculation of the 8 straight lines describing the internal area of the hollow box by a linear regression is completed, see Figure 10. In addition, for each of these regression functions, the distribution function, derived from the topography of the concrete surface and the uncertainty of measurement of the LiDAR is determined. In Figure 15, this is shown schematically for a partial area ($F03^{01}$, gray colored), calculated from the mean values of the distribution function. The regression functions (red lines) with the corresponding distribution functions are shown. In order to calculate the area (Figure 15, $F03^{01}$), the intersection points (red points) of the regression functions must now be calculated. In the next step of the simulation, the position of the 8 straight lines are now varied according to the respective distribution function and an additional area (Figure 15, $F03^{02}$, green colored) is calculated. This variation is represented by green lines and green intersection points in Figure 15.

With this procedure, a sufficient number of surfaces are then calculated. In the performed simulation, this was 100,000 process steps. In each of these process steps, the total area of the cross - section profile is calculated from the partial areas so that a total of 100,000 surfaces are calculated under consideration of the variations.

Figure 16 shows a typical result of the performed Monte-Carlo simulation. The reconstructed 2D model of the cross-section profile can be seen in the right part of the image. The related standard deviation (SD) and the coefficient of determination (R^2) are listed for each edge. If the component edge is displayed in green, the degree of determination is larger than 0.95. If the edge is colored red, it is less than 0.95. This is used to control model formation. The magenta colored points of the point cloud are automatically not considered in the calculation by the algorithm. The histogram of the simulated surface calculations can be seen on the left hand side. From this, the empirical distribution of the surface can now be deduced.

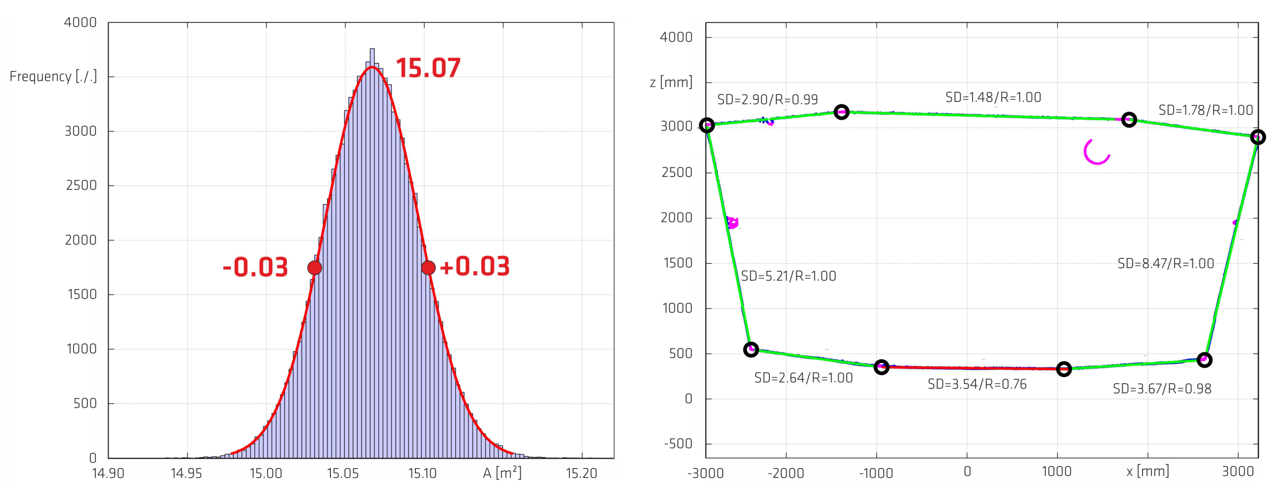

Figure 16: Typical result of the Monte-Carlo simulation for the cross-section profile SP06.

Table 1 lists the results of the Monte-Carlo simulation for the cross-section profile SP06. The slight deviations from the result from [5] are due to a correction in the segmentation of the point cloud.

Table 1: Calculated sub-areas and sum of the sectional plane SP06.

Description	F_M [m²]	SD [m²]
F 01	1.742	0.018
F 02	2.135	0.022
F 03	4.470	0.045
F 04	2.793	0.028
F 05	2.037	0.020
F 06	1.889	0.018
F_{SP06}	**15.067**	**0.028**

After the 27 cross-sections have been evaluated, including NDT measurements, the basis for the calculation of the dead weight of the bridge element has now been created. The calculation assumes that the topography of the concrete surfaces between the profiles does not change significantly. In order to examine this assumption, the volume of the inner hollow box will be calculated by means of a refinement of the segmentation.

Estimation of the internal volume

The inner volume of the hollow box girder is estimated by segmenting it into partial volumes, which are subsequently summed. The Monte-Carlo algorithm developed for 2D modeling is used for this purpose. The basic procedure is shown schematically in Figure 17. For the calculation of the volume, the point cloud is separated into equidistant plane cross-section profiles. This is done with the smallest distance of the profiles of 0.5 m (d, Figure 17). Therefore, a total of 136 segments is used for the calculation. Subsequently, the volume is determined by means of the Monte-Carlo simulation for each cross-section.

Figure 17 shows graphically the procedure for calculating the volume. The point cloud is divided into equidistant areas, Figure 17 (Detail 01). For the first and last profile, only half of the distance (d) to the next profile is considered, Figure 17 (Detail 02). The total volume is obtained from the sum of the different volume segments.

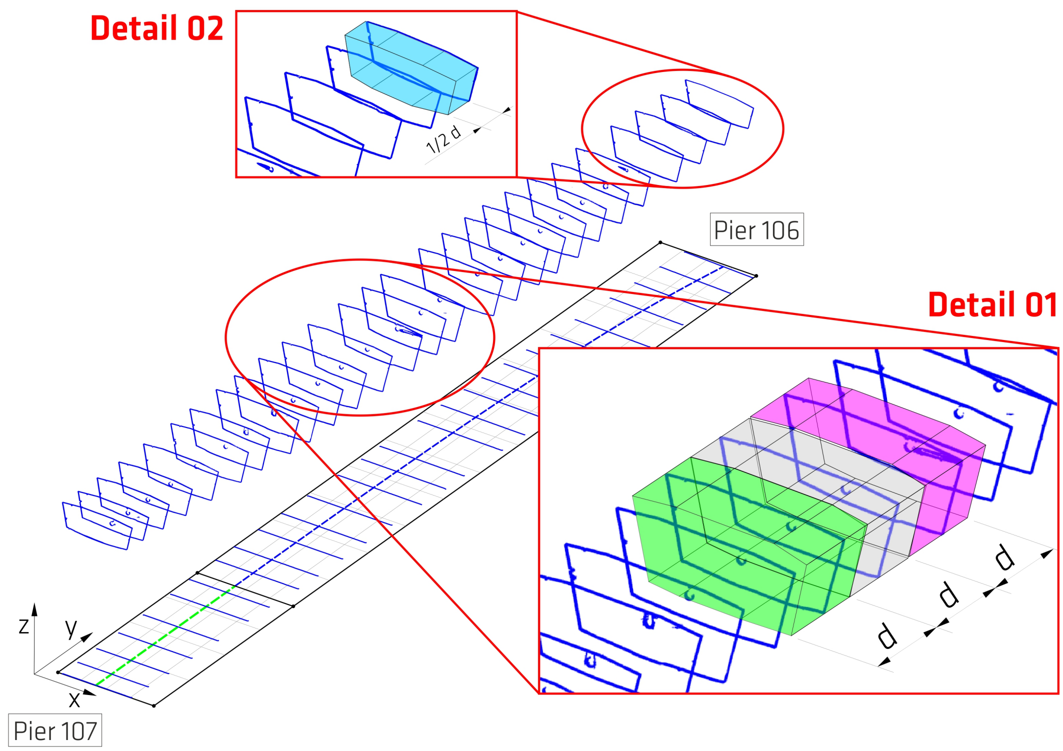

Figure 17: Segmentation of the volume elements for the approximate calculation of the internal volume.

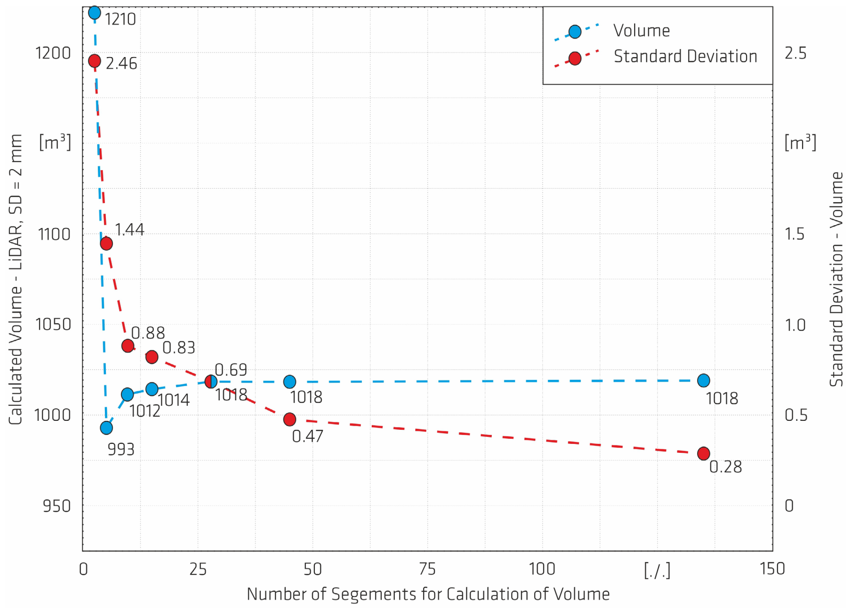

Figure 18: Diagram of the change in the calculated volume and the associated standard deviation as a function of the segmentation of the volume elements with an assumed uncertainty of measurement of ± 2 mm for the LiDAR method.

Figure 18 shows one possible way how to estimate the accuracy of the result of the volume calculation. For this purpose, the partial results of the volume calculation are compared in the diagram. On the lower axis, the number of equidistant volume elements used in the calculation is plotted. On the left axis, the calculated volume is plotted, and on the right axis the standard deviation from the empirically calculated distribution function is plotted. The colored dots pair with the values. The blue dot indicates the volume, while the red dot shows the associated standard deviation. This procedure is similar to an integral calculation. However, because the cross-section profile changes along the axis, the result is significantly different, especially if only a small number of segments is considered.

The diagram shows that the volume reaches a value of 1018 m³ continuously with an increasing number of segments. At the same time, the standard deviation decreases to ±0.28 m³ with falling tendency. From this it can be concluded that the surface of the concrete between the transverse profiles, where the NDT measurements were carried out, do not significantly change.

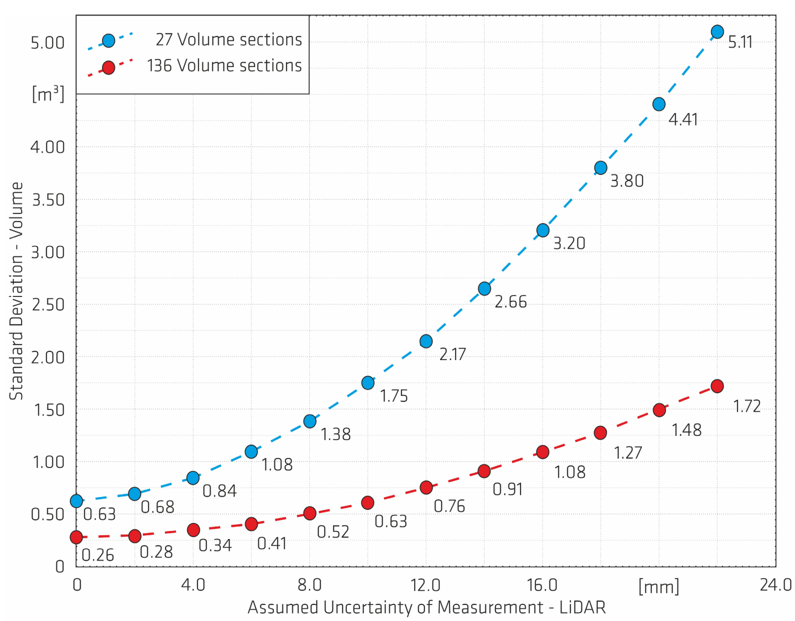

Figure 19: Estimation of the influence of the uncertainty of measurement of the LiDAR method on the calculated internal volume of the bridge element for two cases of the segmentation of the volume.

Estimation of the influence of the uncertainty of measurement of the LiDAR on the volume calculation

The influence of the uncertainty of measurement of the LiDAR data on the volume calculation is estimated by varying the uncertainty of measurement. The variation takes place in increments of ±2 mm up to an assumed uncertainty of ±22 mm. The maximum value of ±22 mm of the assumed uncertainty results not only from the deviations caused by the measuring device. Rather, it is also assumed here that the bridge deforms during the measurements because of the dynamic loads on the traffic or of the wind as a whole. European regulations limit the deformation to f_{max} = L / 1540 [11]. A maximum deformation of about ±45 mm would thus be permissible in the case of the investigated area of the bridge. This maximum value is usually not reached, as other criteria of the calculation are taken into consideration beforehand. Therefore, the assumption of a maximum deformation for a first estimate of ±22 mm appears plausible.

Figure 19 shows the result of the estimation of the influence of the uncertainty of measurement of the LiDAR method on the calculation of the volume. If the measuring uncertainty of the LiDAR method is assumed to be ±0 mm, the value for the standard deviation of ±0.26 mm results solely from the quality of the surface of the concrete. With a larger assumed measurement uncertainty, the variance of the calculated volume increases. This shows a non-linear course. Therefore, it is very easy to see that the influence increases significantly and is thus a major factor in the calculation of the dead weight of the bridge.

Summary

This presentation highlights the results of Step 2 of the research project carried out at BAM in Berlin [4]. The overall objective of the research project is to demonstrate that non-destructive testing procedures can be used to support the recalculation of bridge structures in Germany. With these methods, the dead weight of the bridge can be calculated. The exact knowledge of the dead weight allows a calculational reassessment of the structural integrity of the building.

In order to take advantage of the results of the non-destructive testing, it is necessary to record the geometry of the measuring surfaces in the interior of the structure with sufficient precision. Therefore, the geometry was measured using a spatially scanning LiDAR method. In the first part of this research project [5], the data recording of the internal structure of a region of a hollow box girder was described in detail. Furthermore, the first approaches illustrated how the measurement data can be transferred to a 2D model based on which subsequent recalculation is then carried out.

This presentation explains in detail the creation of a 2D model of the bridge which is obtained from the spatial LiDAR data. The imperfections of the component surface are taken into account by the introduction of a related standard deviation. A 2D model of the cross profiles is then created for the positions where the NDT measurements were made. The calculation is done with the help of a Monte-Carlo simulation. With this simulation technique, it is possible to calculate the area by providing the empirical distribution function.

In order to be able to assess the areas between the modeled cross-section profiles, the volume of the inner hollow box was calculated. For this purpose, a significantly finer segmentation of the hollow box took place. The volume calculation was carried out using the Monte-Carlo simulation. To assess the influence of the different parameters, the influencing values were varied stepwise. The determination of the exact measurement uncertainty of the LiDAR method under the real boundary conditions of the particular building is the subject of further research work.

Acknowledgment

The studies were carried out in the frame of a research project, funded by the Federal Ministry of Economics of Germany (BMVI). We would also like to thank the project partners from WTM Engineers – Hamburg (WTM) and the Hamburg Port Authority (HPA) for giving us the support and the opportunity to carry out the studies at the bridge. The measurements were carried out by order of the HPA in cooperation with the Brandenburg University of Applied Sciences, Department of Informatics and Media.

References

[1] BMVBS: Richtlinie zur Nachrechnung von Straßenbrücken im Bestand (Nachrechnungsrichtlinie) *(Standard for bridge re-analysis and assessment*). Bundesministerium für Verkehr, Bau und Stadtentwicklung (BMVBS) (Federal Ministry of Transport and Digital Infrastructure), 2011, (German).

[2] Haveresch, K.: Nachrechnen und Verstärken älterer Spannbetonbrücken (*Checking and Strengthening older Prestressed Concrete Bridges*). Beton- und Stahlbetonbau 106 (2011), 2, S. 89–102, (German).

[3] DBV Bautechnik Verein e.V.: Beispiele zur Bemessung nach Eurocode 2: Ingenieurbau. Beispiel 13: Plattenbalkenbrücke (*Examples for dimensioning according to Eurocode 2: Civil Engineering. Example 13 Plate Bridge Bridge*). Ernst & Sohn, Berlin, 2015, (German).

[4] Forschungsvorhaben: ZfPStatik – Einbinden der automatisierten zerstörungsfreien Prüfung in die statische Nachrechnung und ganzheitliche Beurteilung bestehender Autobahnbrücken. funded by Bundesministerium für Verkehr, Bau und Stadtentwicklung (BMVBS) (Federal Ministry of Transport and Digital Infrastructure), ongoing project

[5] Knackmuß, J.; Maack, S.; Creutzburg, R.: Comparative visualization of the geometry of a hollow box girder using 3D-LiDAR - Part 1: Cross sectional area. In: Society for Imaging Science and Technology (Hrsg.). Electronic Imaging SCIENCE AND TECHNOLOGY, USA, 2016.

[6] Daniels, D. J.: Ground penetrating radar. Institution of Electrical Engineers, London, 2004.

[7] Braml, T.; Taffe, A.; Feistkorn, S.; Wurzer, O.: Assessment of Existing Structures using Probabilistic Analysis Methods in Combination with Nondestructive Testing Methods. Structural Engineering International 23 (2013), 4, S. 376–385.

[8] Beutel, R.; Reinhardt, H.-W.; Grosse, C. U.; Glaubitt, A.; Krause, M.; Maierhofer, C.; Algernon, D.; Wiggenhauser, H.; Schickert, M.: Comparative Performance Tests and Validation of NDT Methods for Concrete Testing. Journal of Nondestructive Evaluation 27 (2008), 1-3, S. 59–65.

[9] Maierhofer, C.; Krause, M.; Mielentz, F.; Streicher, D.; Milmann, B.; Gardei, A.; Kohl, C.; Wiggenhauser, H.: Complementary Application of Radar, Impact-Echo, and Ultrasonics for Testing Concrete

Structures and Metallic Tendon Ducts. Transportation Research Record 1892 (2004), 1, S. 170–177.

[10] Wiggenhauser, H.; Kind, T.: GPR Investigation of Reinforced-Concrete Structures: Radar for Bridge Condition and Performance Evaluations. Workshop, Washington, 2011.

[11] Roßner, W.: Spannbetontragwerke von Straßenbrücken – Bemessungsvergleich nach neuen Nationalen Normen und bisherigen Europäischen Normen (*Prestressed concrete structures of road bridges – Comparison design of the new National and previous European Standards)*. Bautechnik 84 (2007), 5, S. 301–310. (German)

[12] Braml, T.; Wurzer, O.: Probabilistische Berechnungsverfahren als zusätzlicher Baustein der ganzheitlichen Bewertung von Brücken im Bestand (*Probabilistic analysis methods as an additional component for the integrated assessment of existing bridges*). Beton- und Stahlbetonbau 107 (2012), 10, S. 654–668, (German).

Author Biography

Stefan Maack received his Diploma (2004) and his PhD in civil engineering at Technical University of Berlin in Germany (2012). From 2005 to 2007 he worked in an engineering office as project leader for nondestructive measurement methods. Since 2007 he has worked at the BAM Bundesanstalt für Materialforschung und -prüfung (Federal Institute for Material Research and Testing) in Berlin, Germany. His work has focused on transfer of scientific NDT approaches into practice. Research interest are in acoustic NDT methods with focus on non-contact techniques.